

Effect of concentrations of plasticizers on the sol-gel properties developed from alkoxides precursors

Sandra Raquel Kunst¹, Marielen Longhi¹, Lilian Vanessa Rossa Beltrami^{2*}, Lucas Pandolphi Zini¹, Rosiana Boniatti², Henrique Ribeiro Piaggio Cardoso², Maria Rita Ortega Vega² and Célia de Fraga Malfatti²

¹Centro de Ciências Exatas e Tecnologia – CCET, Universidade de Caxias do Sul – UCS, Caxias do Sul, RS, Brazil

²Laboratório de Pesquisa em Corrosão – LAPEC, Departamento de Metalurgia – DEMET, Universidade Federal do Rio Grande do Sul – UFRGS, Porto Alegre, RS, Brazil

*lvrossa@yahoo.com.br

Abstract

Coatings developed through sol-gel method is presented as an interesting replacement to chromium coating. Sol-gel method present advantages as high purity and excellent distribution of the components. The objective of this work is to synthesize and characterize a film obtained by sol-gel route. The film was prepared with 3-(trimethoxysilylpropyl) methacrylate (TMSPMA), tetraethoxysilane (TEOS) and cerium nitrate, using water and ethanol as solvents. Polyethyleneglycol (PEG) plasticizer was added at four different concentrations. The sol was characterized by techniques of viscosity, thermogravimetric analysis (TGA), X-ray diffraction (XRD) nuclear magnetic resonance spectroscopy (NMR) and Fourier transform infrared spectroscopy (FT-IR). The results showed that tetrafunctional alkoxides condensation was retarded by the plasticizer, forming a compact film. The film with 20 g.L⁻¹ of PEG showed the best electrochemical behavior.

Keywords: *sol-gel, hybrid film, TEOS, TMSPMA, PEG.*

1. Introduction

Coatings prepared through sol-gel method is an ecological innovative technology due to anticorrosive properties of surface protection of metallic substrates, besides interesting properties in mechanic area^[1].

Surface treatments still used in the packing industry are based on chromates, as they provide excellent corrosion resistance. Nontoxic alternatives to pre-treatments was developed in recent years to replace the chromating process. Hybrid films obtained by sol-gel method are a good alternative to suppress the chromate-based process^[2]. However, the industrialization of the sol-gel process requires testing with the real work substrates^[3].

The sol-gel method promotes the polymerization of the precursors alkoxides silicon to forming a crosslinked network in hybrid films. The sol-gel method polymerization reaction is a two-step process. The first step is the hydrolysis of the alkoxy groups; the second step is the silanol condensation to form siloxane bonds.

Furthermore, the sol-gel obtained coating may have a heterogeneous roughness. In this case, it is recommended to coat with a thicker layer in order to improve the barrier effect or to coat a homogeneous and uniform tinplate substrate. That thickness increase may be done in two ways: increasing the number of layers within limits to avoid delamination^[4] or increasing sol viscosity. Sol viscosity can be controlled by temperature variation or by plasticizer addition. Temperature alters the hydrolysis and condensation reactions kinetics^[5].

Hybrid films obtained by the sol-gel method may not be effective barriers against corrosion because they may present defects. To increase barrier protection, plasticizers, such as polymethylmethacrylate (PMMA)^[6] or polyethyleneglycol

(PEG)^[7], have been used to increase coating thickness and to improve the flexibility of the system, which promote the acquisition of uncracked films that can be subjected to mechanical deformation without failure^[8].

Generally, siloxane hybrid films are homogeneous and present good chemical and thermal stability. Additionally, these coatings have excellent barrier properties that improve the corrosion protection of pretreated substrates; these films act primarily as a barrier-type layer between the substrate and the environment. Consequently, they reduce the entry rate of water, electrolytes and oxygen and inhibit the permeation of species to the interface of the metal, which decreases the corrosion rate of the substrate. Accordingly, the degree of hydrophobicity and adhesion to the substrate (formation of strong covalent bonds; MeOSi)^[6,7] are important properties of these films.

The technology of the sol-gel process is widely used to obtain high quality surface protection through simple procedures and with economic viability. Among its advantages, it is possible to mention: (I) the stoichiometry is easy to control and adjust^[9]. (II) The production of a high purity film and with uniform distribution of its components^[10]. (III) The process can be carried out under normal pressure and low temperatures. Along the last decades a large number of hybrid materials has been obtained from the sol-gel process using various polymers and inorganic precursors^[11-13].

In a preliminary study conducted by Kunst et al.^[14], the tinplate was coated with a hybrid film composed of TEOS, TMSPMA, cerium nitrate in a concentration of 0.01 M and PEG 1500 in a concentration of 20 g.L⁻¹. The authors tested the application of the monolayered and bilayered hybrid films

at different cure temperatures. The results showed that the bilayered hybrid film obtained at 60 °C had a higher layer thickness, and the best performance in the electrochemical assays, as well as the most hydrophobic character, in relation to the other samples. For the monolayered systems, the 90°C-cured system showed a lower layer thickness; however, this system showed a more compact, uniform and less porous layer, and presented better electrochemical impedance results, in comparison with the 60 °C-cured samples^[14].

The objective of this work is to prepare a hybrid film obtained from sol constituted by 3-(trimethoxysilylpropyl) methacrylate (TMSPMA) and tetraethoxysilane (TEOS) and with different polyethylene glycol plasticizer concentration (PEG). This paper evaluated the influence of PEG concentration on the sol formulation in the final physical and chemical properties of the films.

2. Experimental

2.1 Synthesis of hybrid films

The hydrolysis reactions were conducted with the silane precursors 3-(trimethoxysilylpropyl) methacrylate ($C_{10}H_{20}SiO_5$, TMSPMA) and tetraethoxysilane ($C_8H_{20}SiO_4$, TEOS), with 0.01 mol.L⁻¹ cerium nitrate (Ce III) addition (approximately 0.5% by weight) as corrosion inhibitor. Ethanol and water were used as solvents.

The hybrid sols used as the coatings were prepared with the following molar ratios: TEOS: TMSPMA = 2:1; H₂O:Si = 3.5:1; ethanol:H₂O= 1:2. Polyethyleneglycol (PEG, 1500 g.mol⁻¹) was added to the sol formulation at four different concentrations: 0, 20, 40, 60 and 80 g.L⁻¹ (TP-0, TP-20, TP-40, TP-60 and TP-80, respectively) and TR is tinplate without coating. Ethanol and water were used as solvents. The hydrolysis time was 24 hours. According to further characterization tests, the hybrid films were prepared on a petri dish or applied by dip-coating, with 10 cm.min⁻¹ removal rate and 5 minutes of immersion. Posteriorly, the samples were thermally cured at 60 °C for 20 minutes in a furnace. Figure 1 presents the flowchart of the process.

2.2 Experimental techniques

Sol viscosity was measured after 24, 48, 72 and 96 hours of hydrolysis by a Brookfield DV2T viscometer with variable rotation and constant temperature (25 °C) for all samples.

The TGA were performed with a 50-Shimadzu TGA instrument over a temperature range from 23 to 700 °C and with a heating rate of 10 °C.min⁻¹ under a nitrogen (N₂) flow rate of 50 mL.min⁻¹.

Free standing films were studied by XRD and FTIR. X-ray diffraction (XRD) analysis was performed on a Shimadzu XRD-6000 X-ray diffractometer, using a 2θ setting between 10° and 55°, with Cu Kα radiation of 1.5406 Å and step of 0.05°. The analysis of Fourier transform infrared spectroscopy (FTIR) was carried out using the attenuated total reflectance (ATR) on Nicolet IS10 Termo Scientific equipment. Each spectrum was obtained by performing 32 scans between 4000 cm⁻¹ and 400 cm⁻¹.

Solid Nuclear Magnetic Resonance (NMR) analysis of the hybrid films was carried out in an Agilent DD2 500/54 with a magnetic field of 11.7 T (500 MHz for 1H). ¹³C and ²⁹Si experiments were conducted. A rotation of 10000 Hz, a pulse of 2.55 μs, a delay of 5 s and a contact time of 7 ms were the parameters for the ¹³C experiment. For ²⁹Si, a rotation of 5000 Hz, a pulse of 3.2 μs, a delay of 5 s and a contact time of 9 ms were set. Furthermore, a liquid ¹³C NMR analysis was performed for a PEG 1500 sample in deuterated chloroform, in an Agilent 400 MR with a magnetic field of 9.4 T (400 MHz for 1H) and using TMS as internal standard.

The infrared spectroscopy measurements were performed using the technique of attenuated total reflectance (ATR), on Nicolet IS10 Termo Scientific equipment. The measurements were performed with the mid-infrared and each spectrum was obtained by performing 32 scans between 4000 cm⁻¹ and 400 cm⁻¹. The spectra were obtained for the films without a substrate (free-standing films).

3. Results and Discussion

3.1 Sol viscosity

The fluid viscosity is regarded as the spontaneous creep or even to flow resistance and is due to internal friction (forces of attraction between molecules). Verification of viscosity is important to assess the integrity of the sol, being a valuable tool in quality control in the industrial field.

Figure 2 shows the variation of viscosity as a function of hydrolysis time samples. An increasing trend of viscosity as a function of the PEG concentration in the sol is observed, in which the TP-80 sample showed the highest viscosity.

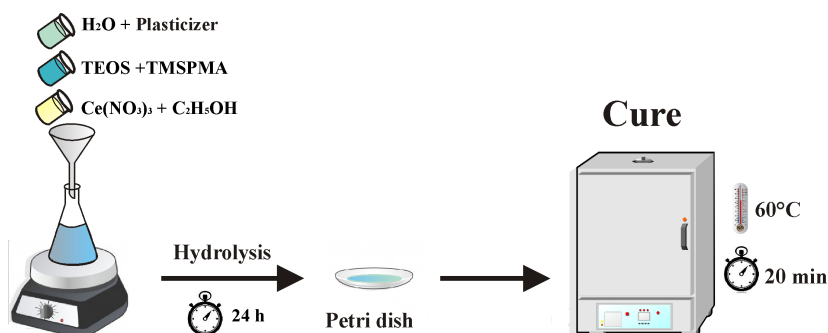


Figure 1. Scheme illustrating the stages of the hybrid films development.

This behavior indicates that the higher the concentration of PEG in the sample, the higher the viscosity.

In addition, the increase of viscosity with time was linear. The sol is a colloidal particles dispersion, that are stable in the fluid, and with time, they become gel formed by the rigid structure of colloidal particles or polymeric chains that immobilizes the liquid phase inside its interstitials^[15]. This transition at room temperature, transforms the sol in gel by setting chemical bonds and molecular interactions between the particles. It allows the formation of a tridimensional solid network that provokes the increase of viscosity in the system up to the gelation point.

As shown in Figure 3, a solution containing water and PEG increases the viscosity gradually with the increase of the PEG concentrations. Low molecular weight PEG is more soluble in water and in nonpolar solvents. Moreover, most silanes hydrolyzable groups have limited solubility in water. Until, though, these groups are converted to hydrophilic silanol groups by hydrolysis. The degree of polymerization of the silanes is determined by the amount of water available and the organic substituent. If the silane is added to water and has low solubility, a degree of polymerization is disfavored and subsequently has a lower viscosity as compared to the polyethylene glycol in aqueous solution^[16,17].

3.2 Thermal characterization

Figure 4 shows the thermograms of TGA of the studied hybrid films and the PEG. For the PEG in Figure 4 is observed only one stage of degradation, with a gradual and uniform weight loss. This event starts from 400 °C and ends at 422 °C. The PEG thermal degradation occurs by thermal cracking of the polymer chain.

The hybrid film without PEG (TP-0) presented a continuous process of weight loss, with a lot of waste at the end of the test. It was observed a loss weight at 110 °C, it was relative at loss of water residual and molecules absorbed in the film. Subsequently, there has been a continuous weight loss up to the end of the test. This event relates to thermal degradation of TEOS and coupled to degradation of TMSPMA, both thermal main chain scission^[18].

For hybrid films with PEG, an influence of the plasticizer on the thermal stability is observed. The addition of PEG improved the thermal stability of the silane coating when compared to the sample without PEG (TP-0). The samples with PEG showed a similar thermal behavior. These results demonstrate that the addition of PEG increases the thermal stability of the hybrid films and that the increase of PEG concentration favors this property.

3.3 Physic-chemical characterization

Figure 5 shows the XRD diffractograms of the studied hybrid films. The silanes do not show arrangements in their crystalline structure, only a broad peak characteristic of the amorphous phase was observed. A gradually increase in the concentration of PEG in the samples is observed in Figure 5, it identified by increase in peak intensity. However, it was not possible to evaluate a change in the crystalline fraction of the hybrid films, since it is not possible to quantitatively compare the change in the intensity of the XRD peaks.

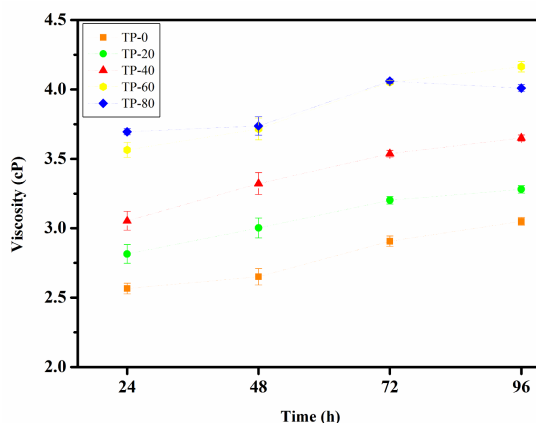


Figure 2. Viscosity at 25 °C for the sols studied with different plasticizer concentrations.

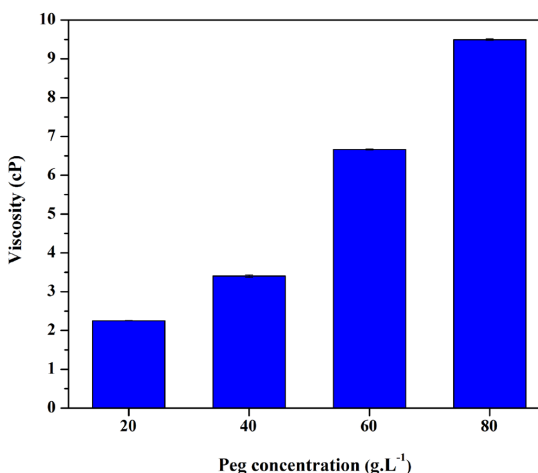


Figure 3. Viscosity at 25 °C, in water after 24 hours, for the solutions containing different PEG concentrations.

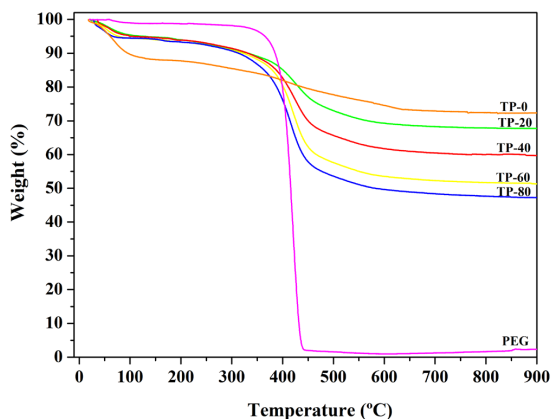


Figure 4. TGA curves of the studied samples and PEG.

Similar results were observed by Yang et al.^[19] in their study on the effect of the concentration of PEG 1500 in composites with SiO₂. The XRD showed that PEG 1500 has the crystalline structure with typical diffraction peaks at 19° and 24° (2θ). When PEG is added in greater concentration in the composite, it promotes a shift in the peak of the amorphous composite, increasing gradually intensity with increasing PEG concentration.

NMR analysis supplies information about the hybrid structures. It was carried out using MestreNova® software. Figure 6 shows the chemical structures of the silane precursors and of the plasticizer. ¹³C and ²⁹Si spectra of the hybrid films appear in Figures 7 and 8. According

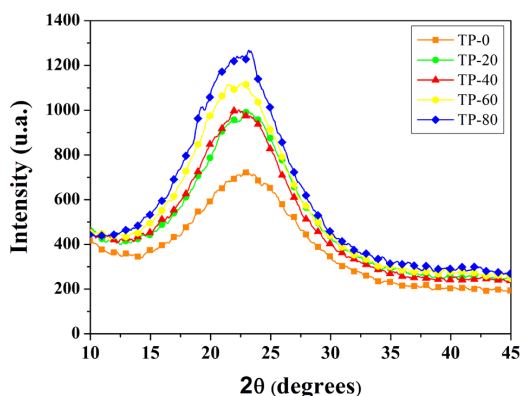


Figure 5. XRD diffractogram of the hybrid films with different PEG concentration.

to ¹³C spectra (Figure 9), there was the formation of ether (C-O-C) function (4 in Figure 6) as the peaks at 66.57 ppm for TP-0 and 69.49 ppm for TP-20, TP-60 and TP-80 indicate (Solomons, 2011). This peak increases its area due to plasticizer addition, since PEG structure corresponds to that of ether, according to ¹³C NMR liquid PEG spectrum (Figure 9).

It is apparent the presence of ester (COOC) function, whose peak is located between 165 and 172 ppm^[20]. This indicates that not all the TMSPMA participated in the hydrolysis process of this group. In addition, this peak area increases with the increase of PEG concentration, which allows us to infer that PEG enables molecular interactions, in this case, hydrogen bonds regarding the oxygen atom presence.

Peaks between 119-140 ppm reveal that the functional group C=CH₂^[20] relates to unpolymerized acrylate structures^[21]. This peak reduces its area with the plasticizer addition.

The different trifunctional (*T*) and tetrafunctional (*Q*) silicon-based structures appear in Figure 10^[21-23]. Table 1 shows the peak localization in ppm for ²⁹Si NMR spectrum of the different *T* and *Q* species present in the hybrid structures. Table 2 shows the polymerization degrees obtained of the hybrid film samples.

Each *T* and *Q* proportion was calculated by integration of the NMR peaks, using MestreNova® software. The relative proportions were calculated as follows (Equations 1 and 2)^[22]:

$$T^i \text{ relative proportion} = \frac{T^i}{\sum T^i} \times 100 \quad (1)$$

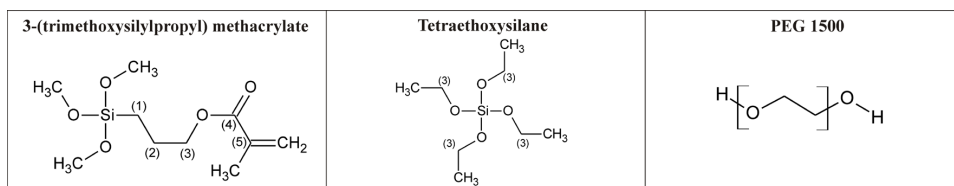


Figure 6. Chemical structures of the silane precursors and the plasticizer.

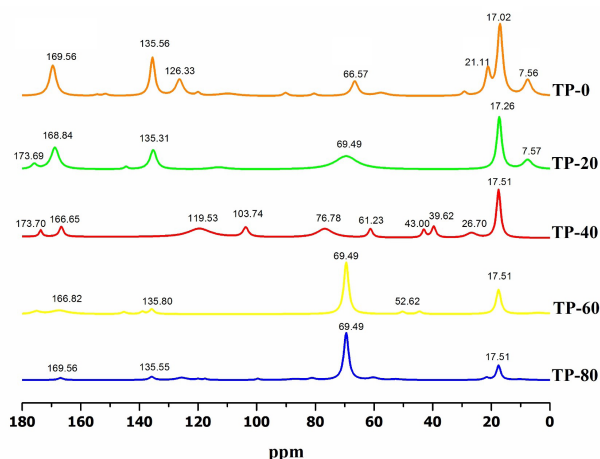


Figure 7. NMR ¹³C spectrum for the hybrid films.

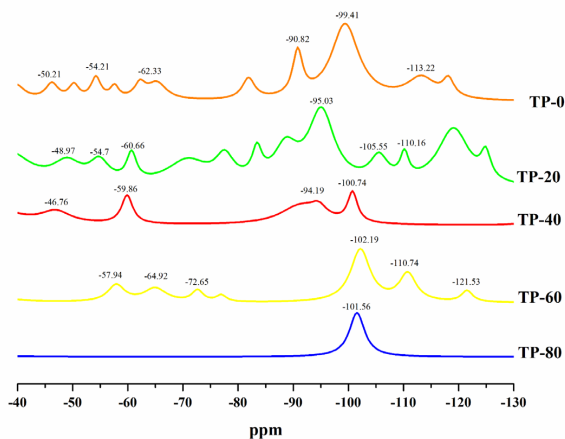


Figure 8. NMR ²⁹Si spectrum for the hybrid films.

Table 1. NMR ²⁹Si peak localization of each silicon-based species in the hybrid films.

Hybrid Film	Peak localization (ppm)					
	T1	T2	T3	Q2	Q3	Q4
TP	-50.21	-54.21	-62.33	-90.82	-99.41	-113.22
TP-20	-48.97	-54.7	-60.66	-95.03	-105.55	-110.16
TP-40	-46.76	-59.86	-	-94.19	-100.74	-
TP-60	-57.94	-64.92	-72.65	-102.19	-110.74	-121.53
TP-80	-	-	-	-	-101.56	-

Table 2. Quantitative analysis for ²⁹Si spectrum.

Hybrid Film	Proportion (%)						Relative proportions						Dc(T) (%)	Dc(Q) (%)	%Ti	%Qi	TDc (%)
	T1	T2	T3	Q2	Q3	Q4	T1	T2	T3	Q2	Q3	Q4					
TP	3.83	8.57	10.33	16.88	40.76	19.63	16.84	37.71	45.45	21.84	52.75	25.41	76.21	75.89	22.73	77.27	75.96
TP-20	14.09	11.42	10.67	42.69	11.74	9.39	38.94	31.56	29.50	66.89	18.39	14.72	63.52	61.96	36.18	63.82	62.52
TP-40	24.69	18.52	0	37.65	19.14	0	57.15	42.86	0	66.30	33.70	0	47.62	58.42	43.21	56.79	53.76
TP-60	11.78	12.42	6.21	41.54	21.41	6.64	38.73	40.85	20.42	59.69	30.77	9.54	60.56	62.46	30.41	69.59	61.88
TP-80	0	0	0	0	100	0	0	0	0	0	100	0	0	75	0	100	75

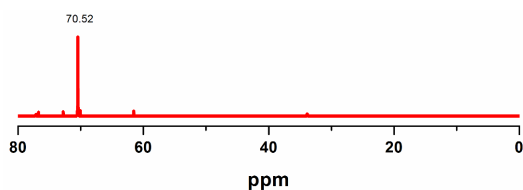


Figure 9. PEG 1500 ¹³C NMR spectrum in liquid phase.

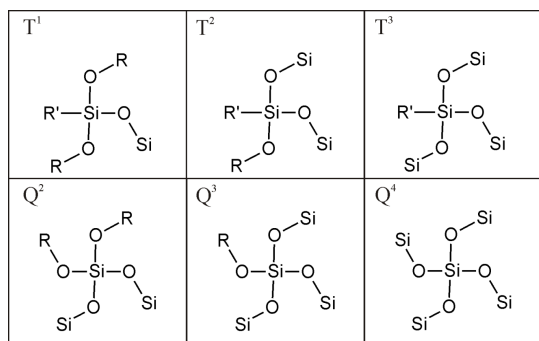


Figure 10. Tⁱ and Qⁱ silicon-based species.

$$Q^i \text{ relative proportion} = \frac{Q^i}{\sum Q^i} \times 100 \quad (2)$$

Polymerization or condensation degree of the trifunctional %Dc(T) and tetrafunctional %Dc(Q) species was calculated using the equations (Equations 3 and 4)^[22,24]:

$$\%D_c(T) = \frac{T^1 + 2T^2 + 3T^3}{3} \times 100 \quad (3)$$

$$\%D_c(Q) = \frac{Q^1 + 2Q^2 + 3Q^3 + 4Q^4}{4} \times 100 \quad (4)$$

The total fractions of trifunctional and tetrafunctional species were calculated as follows (Equations 5 and 6)^[22,24]:

$$\%Ti = \frac{\text{Total T species}}{\text{Total T species} + \text{Total Q species}} \times 100 \quad (5)$$

$$\%Qi = \frac{\text{Total Q species}}{\text{Total T species} + \text{Total Q species}} \times 100 \quad (6)$$

The total degree of condensation corresponds to (Equation 7)^[22,24]:

$$\text{Total } \%D_c = \frac{1}{100} \times \left[(\%D_c(T) \times \%T^i) + (\%D_c(Q) \times \%Q^i) \right] \quad (7)$$

The ²⁹Si spectrum (Figure 8) shows the presence of the different silicon-based species formed in the hybrid films. Both trifunctional (*T*¹) and tetrafunctional (*Q*¹) species were found in the hybrid films, except in the one with the highest PEG concentration (TP-80). Peak values are similar to those found by other authors^[22,23,25,26].

PEG addition diminished the formation of diverse *Q*¹ structures and favored the formation of one of them, in this case *Q*³ structures regarding the peak position close to -100 ppm, and the decrease or absence of other *Q*¹ peaks (Figure 10). On the other hand, PEG addition in concentration up to 60 g.L⁻¹ increased the formation of different *T*¹ structures. Increasing PEG concentration above that value can reduce the *T*¹ structures amount, as the results for sample TP-80 suggest (Table 2).

The sample without PEG addition TP-0 had the lowest *T*¹, *T*² and *%T*¹, as well as the maximum *Q*³, *Q*¹ and *%Q*¹. It can be stated that the addition of plasticizer up to the determined concentration, in this case 40 g.L⁻¹, enhanced the formation of a more flexible structure. In the case of absence of the plasticizer, there was a formation of a more or less condensed structure.

For all hybrid films, except for the TP-80 one, similar polymerization degrees between *T*¹ and *Q*¹ species were observed (Table 2). However, PEG inhibited the complete reaction of all the species in the condensation reactions, since its addition enhanced the formation of *T*¹ species^[22]. Besides, the higher the amount of *T*¹ species the higher the free volume in the polymer.

The addition of a low amount of PEG enhanced an optimal degree of polymerization for the TP-20 sample. The formation of diverse *T*¹ and *Q*¹ structures was promoted by PEG addition. This allowed an optimal compromise between the compactness of *Q*¹ structures that enhances the barrier effect of the film, and the flexibility of *T*¹ species that made the structure more resistant to plastic deformation thus avoiding cracks on the film.

Due to the PEG trend to polymerize in a semi-crystalline form, it is possible to propose that, for TP-60 and TP-80 samples, PEG polymerization during the condensation reactions promoted the formation of a more fragile structure. It explains the increase of the width and the area of peaks at ppm close to 69.49 in ¹³C spectrum. As well as the higher brittleness of sample TP-80.

Figure 11 shows the Fourier transform infrared (FTIR) spectra for all the hybrid films. In all the spectra, strong bands located at 1000 cm⁻¹ and 1200 cm⁻¹ were observed. They are attributed to Si-O-Si bonds and constitute the hybrid structure Backbone. Bands between 900 cm⁻¹ and 960 cm⁻¹ emerge due to the SiOCH₂CH₃, a product of the incomplete TEOS hydrolysis. Bands at 1728 cm⁻¹ and 1622 cm⁻¹ are respectively associated with C=O and C=C stretching. Peaks at 2900 cm⁻¹ are related to symmetric and asymmetric stretching of CH₂

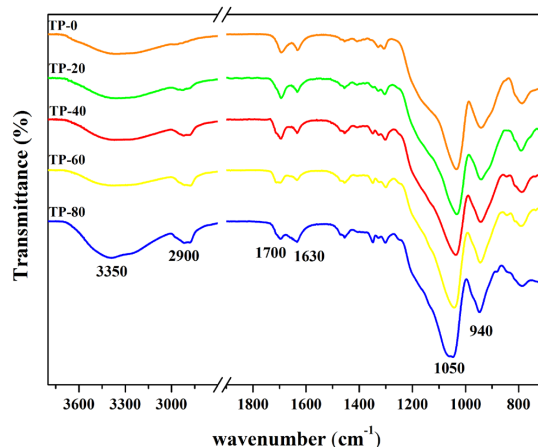


Figure 11. FTIR spectra for the studied hybrid films.

and CH₃ in the TMSPMA aliphatic chain. A wide band between 3200 cm⁻¹ and 3700 cm⁻¹ characteristic of -OH axial deformation is also present^[27], which can arise from silanol groups (Si-OH) that did not condensed during the synthesis process^[28]. This band increased its intensity with the augments of PEG concentration.

4. Conclusions

Results showed that the increase of the *T*¹ was observed by RMN analysis. It promoted the formation of a compact film, enhanced by *Q*² and *Q*³ species, with a high flexibility given by the *T*¹ and *T*² structures.

Regarding the TP-0, according to ²⁹Si NMR spectrum, it possibly could present a good barrier effect behavior, promoted by the presence of more *Q*¹ structures. It was observed by NMR ¹³C spectrum and XRD diffractogram that higher PEG concentrations produced a cross-linked polymer with an important crystalline fraction.

Based on the results, it concluded that the hybrid films showed a good properties with a lower concentration of PEG. Thus, these films may be indicated for coating metal substrates aiming to improve the corrosion protection in many areas of the metals industry.

5. Acknowledgements

The authors would like to thank the Brazilian government agencies CNPq and CAPES for their financial support for this research.

6. References

1. Certhoux, E., Ansart, F., Turq, V., Bonino, J. P., Sobrino, J. M., Garcia, J., & Reby, J. (2013). New sol-gel formulations to increase the barrier effect of a protective coating against the corrosion of steels. *Progress in Organic Coatings*, 76(1), 165-172. <http://dx.doi.org/10.1016/j.porgcoat.2012.09.002>.
2. Hu, H., Li, N., Cheng, J., & Chen, L. (2009). Corrosion behavior of chromium-free dacromet coating in seawater. *Journal of Alloys and Compounds*, 472(1-2), 219-224. <http://dx.doi.org/10.1016/j.jallcom.2008.04.029>.

3. Hansal, W. E. G., Hansal, S., Pözlner, M., Kornherr, A., Zifferer, G., & Nauer, G. E. (2006). Investigation of polysiloxane coatings as corrosion inhibitors of zinc surfaces. *Surface and Coatings Technology*, 200(9), 3056-3063. <http://dx.doi.org/10.1016/j.surfcoat.2005.01.049>.
4. Merlatti, C., Perrin, F. X., Aragon, E., & Margaillan, A. (2008). Evaluation of physico-chemical changes in sub-layers of multi-layer anticorrosive marine paint systems: plasticizer and solvent release. *Progress in Organic Coatings*, 61(1), 53-62. <http://dx.doi.org/10.1016/j.porgcoat.2007.09.001>.
5. Wang, D., & Bierwagen, G. P. (2009). Sol-gel coatings on metals for corrosion protection. *Progress in Organic Coatings*, 64(4), 327-338. <http://dx.doi.org/10.1016/j.porgcoat.2008.08.010>.
6. Zhu, D., & Van Ooij, W. J. (2003). Corrosion protection of AA 2024-T3 by bis-[3-(triethoxysilyl)propyl]tetrasulfide in sodium chloride solution. Part 2: mechanism for corrosion protection. *Corrosion Science*, 45(10), 2177-2197. [http://dx.doi.org/10.1016/S0010-938X\(03\)00061-1](http://dx.doi.org/10.1016/S0010-938X(03)00061-1).
7. Seth, A., Van Ooij, W. J., Puomi, P., Yin, Z., Ashirgade, A., Bafna, S., & Shivane, C. (2007). Novel, one-step, chromate-free coatings containing anticorrosion pigments for metals: an overview and mechanistic study. *Progress in Organic Coatings*, 58(2-3), 136-145. <http://dx.doi.org/10.1016/j.porgcoat.2006.08.030>.
8. Vanin, F. M., Sobral, P. J. A., Menegalli, F. C., Carvalho, R. A., & Habitante, A. M. Q. B. (2005). Effects of plasticizers and their concentrations on thermal and functional properties of gelatin-based films. *Food Hydrocolloids*, 19(5), 899-907. <http://dx.doi.org/10.1016/j.foodhyd.2004.12.003>.
9. Sanchez, C., Julián, B., Belleville, P., & Popall, M. (2005). Applications of hybrid organic-inorganic nanocomposites. *Journal of Materials Chemistry*, 15(35-36), 3559. <http://dx.doi.org/10.1039/b509097k>.
10. Brinker, C. J. (1990). *Sol-gel science: the physics and chemistry of sol-gel processing*. Boston: Academic Press.
11. Martin, J., Hosticka, B., Lattimer, C., & Norris, P. (2001). Mechanical and acoustical properties as a function of PEG concentration in macroporous silica gels. *Journal of Non-Crystalline Solids*, 285(1-3), 222-229. [http://dx.doi.org/10.1016/S0022-3093\(01\)00457-4](http://dx.doi.org/10.1016/S0022-3093(01)00457-4).
12. Oh, C., Do Ki, C., Young Chang, J., & Oh, S.-G. (2005). Preparation of PEG-grafted silica particles using emulsion method. *Materials Letters*, 59(8-9), 929-933. <http://dx.doi.org/10.1016/j.matlet.2004.09.048>.
13. Costa, E. (1998). *Preparação e caracterização de filmes finos sol-gel de Nb₂O₅-TiO₂* (Doctoral thesis). University of São Paulo, São Paulo.
14. Kunst, S. R., Beltrami, L. V. R., Cardoso, H. R. P., Vega, M. R. O., Baldin, E. K. K., Menezes, T. L., & Malfatti, C. F. (2014). Effect of curing temperature and architectural (monolayer and bilayer) of hybrid films modified with polyethylene glycol for the corrosion protection on tinplate. *Materials Research*, 17(4), 1071-1081. <http://dx.doi.org/10.1590/1516-1439.284614>.
15. Hiratsuka, R., Santilli, C., & Pulcinelli, S. (1995). O processo sol-gel: uma visão físico-química. *Química Nova*, 18(2), 171-180. Retrieved in 2016, October 12, from http://quimicanova.sbq.org.br/detalhe_artigo.asp?id=4794
16. Sabadini, E. *Estudo físico-químico de polietileno glicol com água e sorventes aromáticos* (Doctoral thesis). University of Campinas, Campinas.
17. de Oliveira, M. F. (2006). *Estudo da influência de organossilanos na resistência à corrosão de aço-carbono por meio de técnicas eletroquímicas* (Doctoral thesis). University of São Paulo, São Paulo.
18. Pardal, F., Lapinte, V., & Robin, J.-J. (2009). Modification of silica nanoparticles by grafting of copolymers containing organosilane and fluorine moieties. *Journal of Polymer Science. Part A, Polymer Chemistry*, 47(18), 4617-4628. <http://dx.doi.org/10.1002/pola.23513>.
19. Yang, H., Feng, L., Wang, C., Zhao, W., & Li, X. (2012). Confinement effect of SiO₂ framework on phase change of PEG in shape-stabilized PEG/SiO₂ composites. *European Polymer Journal*, 48(4), 803-810. <http://dx.doi.org/10.1016/j.eurpolymj.2012.01.016>.
20. Solomons, T. W. G. (2011). *Organic chemistry*. Hoboken: Wiley.
21. Suegama, P. H., Sarmiento, V. H. V., Montemor, M. F., Benedetti, A. V., de Melo, H. G., Aoki, I. V., & Santilli, C. V. (2010). Effect of cerium (IV) ions on the anticorrosion properties of siloxane-poly(methyl methacrylate) based film applied on tin coated steel. *Electrochimica Acta*, 55(18), 5100-5109. <http://dx.doi.org/10.1016/j.electacta.2010.04.002>.
22. Han, Y.-H., Taylor, A., Mantle, M. D., & Knowles, K. M. (2007). UV curing of organic-inorganic hybrid coating materials. *Journal of Sol-Gel Science and Technology*, 43(1), 111-123. <http://dx.doi.org/10.1007/s10971-007-1544-8>.
23. Cambon, J.-B., Esteban, J., Ansart, F., Bonino, J.-P., Turq, V., Santagneli, S. H., Santilli, C. V., & Pulcinelli, S. H. (2012). Effect of cerium on structure modifications of a hybrid sol-gel coating, its mechanical properties and anti-corrosion behavior. *Materials Research Bulletin*, 47(11), 3170-3176. <http://dx.doi.org/10.1016/j.materresbull.2012.08.034>.
24. Chang, T. C., Wang, Y. T., Hong, Y. S., & Chiu, Y. S. (2010). Organic-inorganic hybrid materials. V. Dynamics and degradation of poly(methyl methacrylate) silica hybrids. *Journal of Polymer Science. Part A, Polymer Chemistry*, 38(11), 1972-1980. [http://dx.doi.org/10.1002/\(SICI\)1099-0518\(20000601\)38:11<1972::AID-POLA60>3.0.CO;2-5](http://dx.doi.org/10.1002/(SICI)1099-0518(20000601)38:11<1972::AID-POLA60>3.0.CO;2-5).
25. Yu, Y.-Y., Chen, C.-Y., & Chen, W.-C. (2003). Synthesis and characterization of organic-inorganic hybrid thin films from poly(acrylic) and monodispersed colloidal silica. *Polymer*, 44(3), 593-601. [http://dx.doi.org/10.1016/S0032-3861\(02\)00824-8](http://dx.doi.org/10.1016/S0032-3861(02)00824-8).
26. Mohseni, M., Bastani, S., & Jannesari, A. (2014). Influence of silane structure on curing behavior and surface properties of sol-gel based UV-curable organic-inorganic hybrid coatings. *Progress in Organic Coatings*, 77(7), 1191-1199. <http://dx.doi.org/10.1016/j.porgcoat.2014.04.008>.
27. Stuart, B. (2004). *Infrared spectroscopy: fundamentals and applications*. Chichester: John Wiley & Sons.
28. Flis, J., & Kanoza, M. (2006). Electrochemical and surface analytical study of vinyl-triethoxy silane films on iron after exposure to air. *Electrochimica Acta*, 51(11), 2338-2345. <http://dx.doi.org/10.1016/j.electacta.2005.01.065>.

Received: Oct. 12, 2016

Revised: Mar. 23, 2017

Accepted: Apr. 09, 2017